A Way to Understand Dynamics of Infantile Myoclonic Encephalopathy

Vishal Verma[1,✉]

[1]Indian Institute of Technology Delhi, Hauz Khas, New Delhi, Delhi-110016, India

The goal of this paper is to introduce scientists (especially, paediatrics) to the mathematics that may help understand the dynamics of metabolic epilepsies like glycine encephalopathies quantitatively. The methods include the Wilson Cowan Model coupled with an adaptive control system and the neural energy consumption calculations available in the literature. The present study applies the Liu & Ching and Buxton *et al*. The Liu Sing model, a model for anaesthesia, if optimally parameterized, may prove useful in modelling the Suppression Burst (SB) in Neonatal Myoclonic Encephalopathy (NME).

Cerebral Metabolism/Energy | Population Neurobiology | Epilepsy | Wilson Cowan Model

Correspondence: ***vv0747970@gmail.com***

Introduction

Neonatal Myoclonic seizures represent a complex and often challenging neurological phenomenon observed in the delicate early stages of life. As a subset of neonatal seizures, they present a unique clinical entity characterized by sudden, brief, and often repetitive muscle contractions, typically manifesting within the first few days to weeks of life. These seizures, while rare, demand meticulous attention and swift intervention due to their potential to cause significant morbidity and mortality if left unaddressed.

The etiology of neonatal myoclonic seizures is multifactorial, encompassing a spectrum of underlying neurological disorders, metabolic disturbances, and in some cases, idiopathic origins. This heterogeneity underscores the intricacy of diagnosis and management, necessitating a comprehensive approach that integrates clinical evaluation, neuroimaging studies, and laboratory investigations to elucidate the underlying cause.

Clinically, neonatal myoclonic seizures often present as sudden jerking movements, typically involving the extremities, face, or trunk, which may occur spontaneously or be triggered by external stimuli. Distinguishing these seizures from other neonatal paroxysmal events such as benign sleep myoclonus or jitteriness requires astute clinical acumen and careful observation.

In addition to the immediate clinical challenges posed by neonatal myoclonic seizures, there are broader implications for the long-term neurological development and overall prognosis of affected infants. The potential for adverse neurodevelopmental outcomes underscores the critical importance of prompt diagnosis and initiation of appropriate therapeutic interventions aimed at seizure control and minimizing neurological sequelae.

In this discourse, I aim to explore the intricate landscape of neonatal myoclonic seizures, delving into their clinical presentation, underlying pathophysiology, diagnostic approach, and contemporary management strategies. By illuminating the complexities inherent in this neurological condition, I endeavour to foster a deeper understanding among healthcare practitioners, ultimately enhancing the care and outcomes of infants grappling with this formidable challenge.

The electroencephalogram (EEG) pattern in neonatal myoclonic seizures serves as a crucial diagnostic tool, providing insights into the underlying neurophysiological abnormalities associated with this condition. In neonates experiencing myoclonic seizures, the EEG typically reveals characteristic patterns indicative of abnormal neuronal discharges. These patterns often manifest as high-voltage, generalized polyspike and wave complexes, frequently occurring synchronously with the myoclonic jerks. Additionally, background abnormalities such as burst suppression, discontinuity, or abnormal sleep architecture may be observed, reflecting the underlying neurological dysfunction, for example, see (1) and (2). The presence of these distinct EEG signatures aids in confirming the diagnosis of neonatal myoclonic seizures, guiding therapeutic interventions, and monitoring treatment response. Understanding the nuances of EEG patterns in neonatal myoclonic seizures is essential for clinicians involved in the care of affected infants, facilitating accurate diagnosis and tailored management strategies aimed at optimizing neurodevelopmental outcomes.

Nonketotic hyperglycemia, also known as hyperglycemic hyperosmolar state (HHS), represents a critical metabolic derangement characterized by severe hyperglycemia and hyperosmolality in the absence of significant ketoacidosis. This condition primarily affects individuals with poorly controlled diabetes mellitus, particularly type 2 diabetes, and is often precipitated by factors such as infection, medication noncompliance, or underlying medical conditions. Unlike diabetic ketoacidosis (DKA), HHS is marked by profound dehydration and hyperosmolality, leading to neurologic symptoms such as altered mental status, seizures, and coma. Prompt recognition and aggressive management are imperative to mitigate the potentially life-threatening complications associated with nonketotic hyperglycemia. A comprehensive understanding of its pathophysiology, clinical presentation, and management principles is essential for healthcare practitioners to effectively diagnose, treat, and prevent the devastating consequences of this metabolic emergency.

Epilepsy stands as a complex neuropathophysiological con-

DRAFT

dition, stemming from the intricate disruption of Excitation-Inhibition Homeostasis (E-I Homeostasis) within neural networks. Within this dynamic framework, the delicate balance between excitatory and inhibitory forces is perturbed, leading to a state where excitation predominates over inhibition, resulting in hyper-synchronized firing of excitatory neural populations. This dysregulation precipitates a myriad of seizure manifestations, each with its distinct etiology rooted in neural and synaptic abnormalities. Consequently, a plethora of modelling endeavours has emerged, seeking to elucidate the underlying causes and mechanisms driving epileptic seizures. Notably, a significant portion of mathematical and computational investigations delve into the disruption of E-I Homeostasis, employing the neural population model pioneered by Hugh D. Wilson and Jack Cowan in 1972. These studies endeavour to mitigate seizure activity by modulating intrinsic and synaptic homeostasis. Pertinent examples include the works cited, such as those by (3), (4), (5), (6), (7), and (8).

In recent years, the realm of mathematical biology has witnessed a notable expansion, with researchers increasingly integrating additional variables such as blood and oxygen supply dynamics into their investigations. This multidimensional approach aims to provide a more comprehensive understanding of physiological phenomena, bridging the gap between theoretical modelling and experimental observations. Noteworthy examples include the seminal works highlighted in the literature, such as those referenced by (9) and (10).

Experimental findings have underscored the pivotal role of blood and oxygen supply in shaping electroencephalogram (EEG) patterns, particularly evident in the emergence of suppression-burst (SB) patterns. These distinctive EEG signatures coincide with disruptions in the delicate equilibrium between cerebral metabolism and energy demand, as observed in conditions like glycine encephalopathy, also known as nonketotic hyperglycemia (NKH). This rare neonatal myoclonic encephalopathy, rooted in metabolic disorders, can manifest as either a chronic condition or evolve into Lennox Gastaut Syndrome over time. While SB patterns are also observed in Otahara syndrome, a non-metabolic disorder, its discussion lies beyond the scope of this discourse. Despite its rarity, neonatal myoclonic encephalopathy holds the potential for cure in select cases, highlighting the imperative for continued research efforts aimed at unravelling its pathophysiological intricacies.

In 2013, Dulac postulated that delving into the intricacies of energy dysregulation inherent in infantile myoclonic encephalopathy could pave the way towards discovering potential treatments, and, is also a popular topic of discussion, see (2) and (11). In the context of nonketotic hyperglycemia (NKH), where cerebral metabolism falters in providing energy to neurons due to the inability to utilize glycine effectively, a key energy substrate, distinctive suppression-burst (SB) patterns emerge in the electroencephalogram (EEG) of afflicted individuals. However, the precise dynamical mechanism underpinning the formation of these EEG patterns remains elusive. This study endeavours to elucidate how such EEG patterns arise as a consequence of the intricate slow-fast dynamical processes occurring within the brain.

Author's Summary The Wilson Cowan model (WC) has emerged as a powerful tool in deciphering epileptic seizures, rooted in the disruption of Excitation-Inhibition (E-I) homeostasis, which entails depolarization block of interneurons. Moreover, the WC model has contributed significantly to unravelling potential therapeutic interventions or activity modulation strategies (3, 4, 6). Furthermore, it has played a pivotal role in elucidating the progression from focal epileptic seizures to generalized seizures (12). By leveraging the insights gleaned from WC modelling, this study aims to shed light on the intricate dynamics governing SB EEG patterns in NKH, thereby contributing to a deeper understanding of this enigmatic neurological phenomenon and potentially opening avenues for targeted therapeutic interventions.

Author's Synopsis

The current study delves into the intricacies of neural dynamics, leveraging the Liu Shing model—a derivative of the Wilson Cowan model (WC) renowned for its application in understanding brain dynamics during anaesthesia (13). Drawing upon recent data elucidated by Buxton (14), I intricately incorporate an energy supply-demand loop into the WC framework, thus enabling the modelling of a localized brain region reliant on an isolated energy source. Through this novel approach, I successfully replicate the emergence of suppression-burst (SB) patterns in response to heightened energy demands within the neural population.

This investigation underscores the critical interplay between intrinsic and synaptic homeostasis, coupled with the dynamics of the energy-supply demand loop, in engendering the characteristic polyspike activity interspersed with isoelectric silence—a hallmark of SB patterns. Furthermore, I extend this modelling framework to simulate myoclonic encephalopathy within the mouse brain network, employing the Allen Mouse Brain Network Atlas for comprehensive analysis.

In essence, this article offers a holistic perspective on modelling SB patterns characteristic of infantile epilepsy, shedding light on the intricate mechanisms underlying seizures precipitated by deficiencies in oxygen, blood supply, glycine metabolism, and other vital factors.

Model Formulation

In a recent work (15), it was shown through the example of the neural network model that the slow fast subsystem is formulated by adding a modulation variable which evolves on a slower timescale to the fast subsystem as a dynamical input. Here, I add a slow modulating variable to the fast excitatory neural firing to the excitatory node of the Wilson Cowan Model (WC) for my study. As per the WC model, the firing rates of the excitatory-inhibitory neural populations in a brain region are given as:

$$\tau_E \frac{dE}{dt} = -E + (k_E - r_E E) \cdot S(x_E) \quad \textbf{(1)}$$

$$\tau_I \frac{dI}{dt} = -E + (k_I - r_I E) \cdot S(x_I) \quad \textbf{(2)}$$

DRAFT

$$S(x_i) = \frac{1}{1+exp(-a(x_i-\theta))} - \frac{1}{1+exp(a\theta)} \quad \textbf{(3)}$$

$$x_E = c_1E - c_2I + P + \Phi \quad \textbf{(4)}$$

$$x_I = c_3E - c_4I + Q \quad \textbf{(5)}$$

τ_i for $i = E, I$ are timescales for excitatory and inhibitory neural populations. c_j where $j = 1,2,3,4$ are synaptic weights. P_i for $i = 1,2,3,4$ are synaptic biases with only $P_1 \neq 0$. The $S_i(x)$ is called the Firing Rate function and is a sigmoid function. a and θ determine the slope and tuning of the sigmoid respectively. The modification brought in by the addition of the slow varying modulation variable Φ as a current/stimulus into the excitatory population; depending upon the energy consumption-demand of the system results in a slow fast dynamical system. The dynamics of this variable shall be decided by the slow subsystem mimicking a cyclic physiological process such as cerebral metabolism. Firstly, energy consumed per neural population needs to be calculated. This shall depend upon the energy required for the synaptic transmission and neural firing. Thus, the term that measures the firing rate's exponential decay, viz., $-E/\tau_i$ contribution needs not to be included. Only the second term on the right-hand side of equations (1) and (2), F_i, that measures firing rate increment is needed. Such a reasoning leads to the following calculation (14):
If S_{EE}, S_{EI}, S_{IE}, S_{II} are the synaptic currents to excitatory from excitatory to excitatory from inhibitory, to inhibitory from excitatory and from inhibitory to inhibitory neural populations; then, following is true.

$$\frac{A_E}{A_0} = 0.25 + 0.06F_E + 0.31\frac{S_{IE}}{S_{EI}} + 0.053\frac{S_{EI}+S_{IE}}{S_0} \quad \textbf{(6)}$$

$$\frac{A_I}{A_0} = 0.25 + 0.06F_I + 0.31\frac{S_{IE}}{S_{EI}} + 0.053\frac{S_{EI}+S_{IE}}{S_0} \quad \textbf{(7)}$$

A_0 is the average amount of energy consumed per neuron in ATP molecules per second. As per the calculations performed by Herculano Houzel, this value is nearly 2×10^9 ATP/s-neuron regardless of the organism (16). Because the 0.8 fraction of the total neural population in the brain is constituted by excitatory neurons and 0.2 fraction is by inhibitory population; the total energy consumption per population is calculated (ignoring the changes included by the densities and variety that varies from organism to organism) is

$$A = 0.8A_E + 0.2A_I \;\; for \;\; A_0 = 1 \quad \textbf{(8)}$$

Clearly, depending upon variations in timescales τ_i and synaptic weights, the rate of energy consumption shall vary from population to population. These parameters serve as the dual homeostasis control parameters; that account for intrinsic and synaptic homeostasis in the neural populations. Hypothetically, variations in these lead to variations in

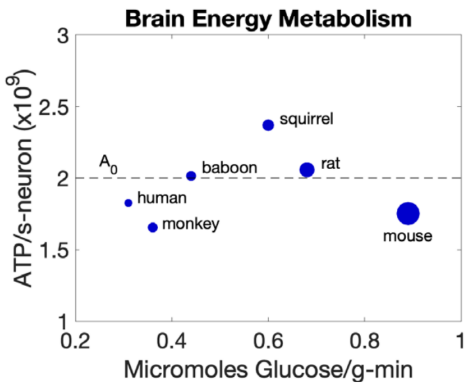

Fig. 1. Energy Consumption of neurons of different organisms in terms of ATP/neuron-s.(16)(14)

the energy demand/consumption. During epilepsy, the excitation firing rate (firing per second) exceeds the normal bounds, as the constituents fire hypersynchronously; while the remaining 20 percent of the inhibitory population firing rate lies low. Consequently, energy demand increases. Thus, the slope $\frac{dA}{dt}$ is more for the epileptic populations than normal populations in the following example. The number of excitatory spikes per second in an isolated healthy mouse brain region, if taken at 8 spikes per second, (14) for reference, the epileptic excitatory firing rate exceeds its count par 20/s.
Figure needed here
Further on, I set a limit on the energy consumption of the neurons in the unit of ATP/neuron-s as a measure to control (as shown biologically (16)). This limit is on $\frac{dA}{dt}$. If it exceeds such that, the rate of consumption exceeds 2×10^9, the cerebral metabolism shall exhibit cyclic dynamics. As the resource (say, extracted from glycine) is consumed, metabolism shall enter a recovery/refill phase. This shall be cyclic, as long as the population remains epileptic owing to disruption in its dual Homeostasis. Even if the population's dual homeostasis is fine and the energy metabolism is slow to meet the energy needs of the population; as in the case of glycine encephalopathy and neonatal metabolic myoclonic encephalopathy; the same dynamic mechanism shall be underway.
Now, I proceed to include a cyclic dynamical process for Φ's evolution (13).

$$\frac{d\Phi}{dt} = -f_1 \cdot \phi + f_2 \cdot \frac{1}{\kappa_\Phi(1+exp(\mathcal{G}-\eta))} \quad \textbf{(9)}$$

$\mathcal{G}$ is the substrate left for consumption and η is the threshold value above which it must be for the consumption process. f_1 and f_2 are the time scales or rates for exponential decay and the step-up function respectively. η is also the threshold of the step-up function. κ_Φ sets the width of the step function. Now, dynamics of the $\mathcal{G}$ is given as;

$$\frac{d\mathcal{G}}{dt} = +\kappa_{recovery}\beta - \kappa_{consumption}\left(\frac{1}{1+(\frac{0.1}{0.8E+0.2I})^2}\right) \quad \textbf{(10)}$$

DRAFT

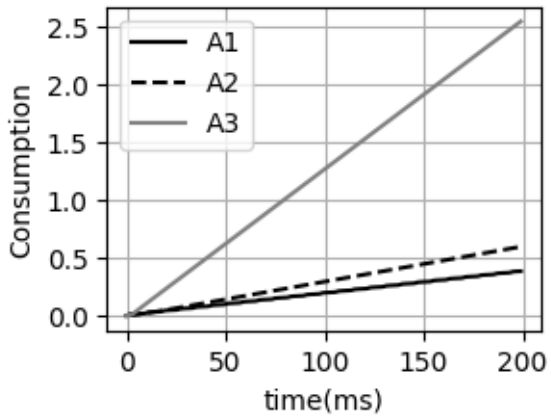

Fig. 2. The More the slope for consumption, the higher the firing rates are. Here, $\frac{dA3}{dt} > \frac{dA2}{dt} > \frac{dA1}{dt}$

As obvious from the equation above, the recovery happens linearly with a slope $\kappa_{recovery}$ with increase in recovery variable β. The consumption, that leads to the decrease in the resource $\mathcal{G}$ starts from zero, and happens monotonically up to a point of saturation $\kappa_{consumption}$. See Appendix A. The recovery dynamics is

$$\frac{d\beta}{dt} = -\rho_1\beta + \rho_2 \cdot \frac{1}{1+exp(-\kappa_{beta}((0.8E-0.2I)-\zeta))} \quad \textbf{(11)}$$

Here again, the first term shows an exponential decay of the recovery of the substrate at all steps, except, when the firing jumped above some threshold ζ decided by the energy consumption A. At this point, the recovery begins (as shown by the step-up function) in the second term on the right-hand side. ρ_1 and ρ_2 are two unequal time scales. κ_{beta} is for the tuning of the step function to set its width.

This slow metabolic process powering Φ establishes a Supply Demand Loop. As the substrate or leftover energy drops below a certain threshold level rapidly due to the increased demand owing to hypersynchronous excitatory firing, the supply Φ stops, and the firing drops; appearing as *suppression*. Or, as the cerebral metabolism is unable to meet the needs of the population firing; owing to the metabolic dysfunction as in (IME), the firing is suppressed as the Φ vanishes. This is shown in the section ().

Results

During metabolic encephalopathies in infants, the delicate balance of dual homeostasis, encompassing both synaptic and intrinsic mechanisms, may operate efficiently, delineated by distinct timescales τ's and synaptic weights c's in equations (1) and (2). However, the sluggish cerebral metabolism inexorably propels the neural population towards burst suppression—a notable feature accurately captured in the model through parameters $\kappa_{consumption}$ and $\kappa_{recovery}$ in equation (10). The spiking rate can be adjusted using τ_E and τ_I.

Synaptic connections, particularly contralateral connections linking neurons across different brain regions, are characterized by elongated lengths. To minimize energy expenditure during synaptic transmissions, such connections exhibit a sparse distribution. Conversely, ipsilateral connections within the same brain region are abundant, as depicted in the adjacency matrix in Figure (6) in left. Furthermore, brain regions interconnected via more synaptic pathways tend to synchronize more readily. Consequently, during activation, these regions form synchronized clusters or colonies, discerned through the Louvain algorithm as illustrated in Figure (6) on the right. Data about the mouse brain connectivity matrix is taken from the Allen mouse brain atlas (see section () Methods).

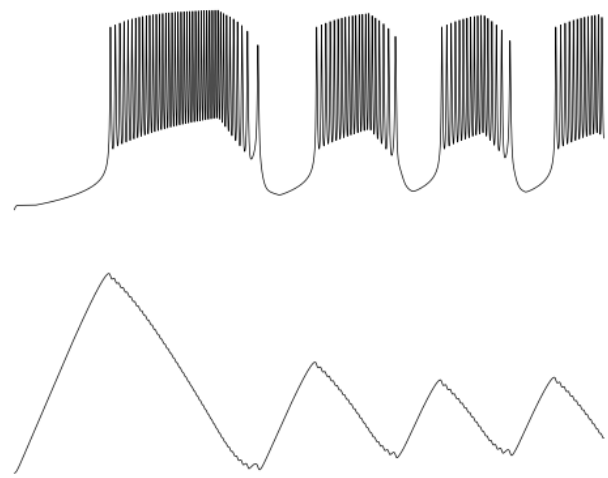

Fig. 3. High excitatory neural firing is driven by oscillations in cerebral metabolism.

Atop this neural hierarchy, a generalized epileptic seizure manifests, characterized by the hyper-synchronous firing of select neurons inducing SB, while others remain silent—a phenomenon intricately linked to the hierarchical structure of the Mouse Brain Network (MBN) and the synaptic strengths modelled herein. See Figure (5). Since the mouse brain network is a small world network, it is not surprising that this pattern can be obtained in other small world nets defined by different numbers of nodes, average path lengths and clustering coefficients, like the human brain. This physiologically corresponds to anaesthesia, Neonatal Myoclonic Encephalopathy (NME) and Nonketotic Hyperglycemia (NKG) though, not the activity patterns that do not involve metabolism malfunction. The parameters make the model show SB with increasing inhibition. This may be unsuitable in the case of epilepsy. However, proper optimization can adjust the model's phase space as per the neurophysiology.

Code Availability

The code for figure 4 and related figures is available on GitHub Myoclonus. Allen mouse brain atlas is publicly available at this link.

Bibliography

1. S. Yoshitomia and et al. Different types of suppression-burst patterns in patients with epilepsy of infancy with migrating focal seizures (eimfs). *Seizure: European J. of Epilepsy*, 65:118–123, 2019. doi: https://doi.org/10.1016/j.seizure.2019.01.009.

DRAFT

2. O. Dulac, M. Lassonde, and H. B. Sarnat, editors. *Pediatric Neurology Part III*. Elsevier, Netherlands, 2013.
3. J. Cannon and P. Miller. Modeling Focal Epileptic Activity in the Wilson–cowan Model with Depolarization Block. *Journal of Math. Neuro.*, 5(7), 2015. doi: 10.1186/s13408-015-0019-4.
4. C. Kim and D. Q. Nykamp. The influence of depolarization block on seizure-like activity in networks of excitatory and inhibitory neurons. *J Comput Neurosci*, 43:65–79, 2017. doi: 10.1007/s10827-017-0647-7.
5. Y. Wang, Taylor P. N. Goodfellow, M., and G. Baier. Dynamic Mechanisms of Neocortical Focal Seizure Onset. *PLoS Comput Biol*, 78, 2014. doi: 10.1371/journal.pcbi.1003787.
6. Tsakalis K. Chakravarthy, N., S Sabesan, and L. Iasemedias. Homeostasis of brain dynamics in epilepsy: A feedback control systems perspective of seizures. *Annals of Biomedical Engineering*, 37(3):565–585, 2009. doi: 10.1007/s10439-008-9625-6.
7. J. Cannon and P. Miller. Stable control of firing rate mean and variance by dual homeostatic mechanisms. *Journal of Math. Neuro.*, 7(1), 2017. doi: 10.1186/s13408-017-0043-7.
8. Y. Wang, M. Goodfellow, P. N. Taylor, and G. Baier. Phase space approach for modeling of epileptic dynamics. *Physical Review E*, 85, 2012. doi: 10.1103/PhysRevE.85.061918.
9. J. Ingram and et al. Oxygen and seizure dynamics: I. Experiments. *J. Neurophysiol.*, 112: 205–212, 2014. doi: 10.1152/jn.00540.2013.
10. Y. Wei, G. Ullah, J. Ingram, and S. J. Schiff. Oxygen and seizure dynamics: Ii. Computational modeling. *J. Neurophysiol.*, 112:213–223, 2014. doi: 10.1152/jn.00541.2013.
11. Y. Fei and et. al. Metabolic control of epilepsy: A promising therapeutic target for epilepsy. *Front. Neurol.*, 11:118–123, 2020. doi: doi.org/10.3389/fneur.2020.592514.
12. S. Ching, B. Emery, and K. Mark. Distributed control in a mean-field cortical network model: Implications for seizure suppression. *Phys. Rev. E*, 86:65–79, 2012. doi: 10.1371/journal.pone.0017514.
13. S. Liu and S. Ching. Homeostatic dynamics, hysteresis and synchronization in a low-dimensional model of burst suppression. *Journal of Math. Bio.*, 74:1011–1035, 2015. doi: 10.1007/s00285-016-1048-7.
14. R. B. Buxton and E. C. Wong. Metabolic energetics underlying neural models. *J. Neurophysiol.*, 112:205–212, 2014. doi: 10.1152/jn.00540.2013.
15. V. Verma. What Causes Persistent Neural Activity? Part I. 2024. doi: 10.1101/2024.02.19.581018.
16. S. Herculano-Houzel. Scaling of brain metabolism with a fixed energy budget per neuron: implications for neuronal activity, plasticity and evolution. *PLoS One*, 6(3):e17514:65–79, 2011. doi: 10.1371/journal.pone.0017514.

DRAFT

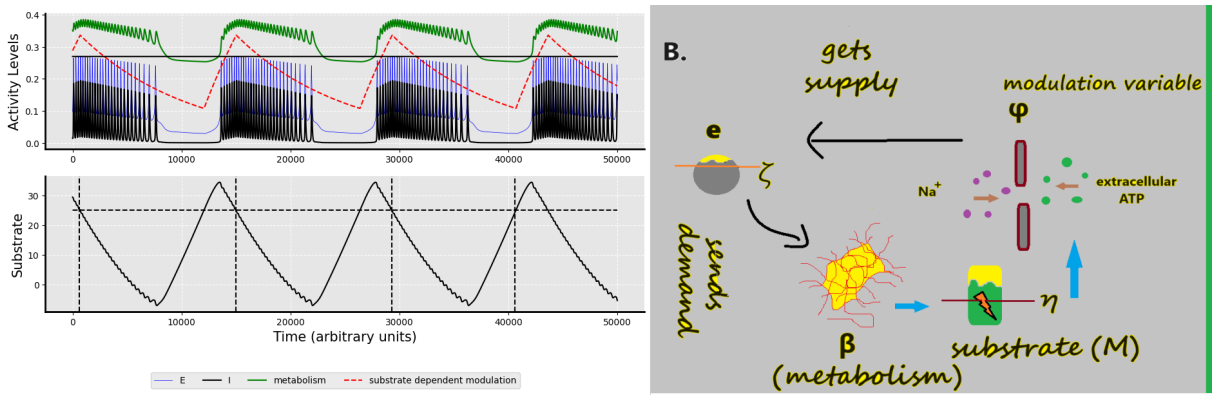

Fig. 4. The excitatory firing rate and inhibitory firing rates are oscillating obeying $E > I$. The black horizontal line, from which blue E bounced down sets the threshold η owing to the energy supply limitations. Φ (red) is oscillating in sync with the oscillations of the available substrate. Metabolic recovery β (green) depends upon the instantaneous firing rate. Burst and suppression pattern *emerge*. Parameters used are same as in (13) and Code Availability section.

DRAFT

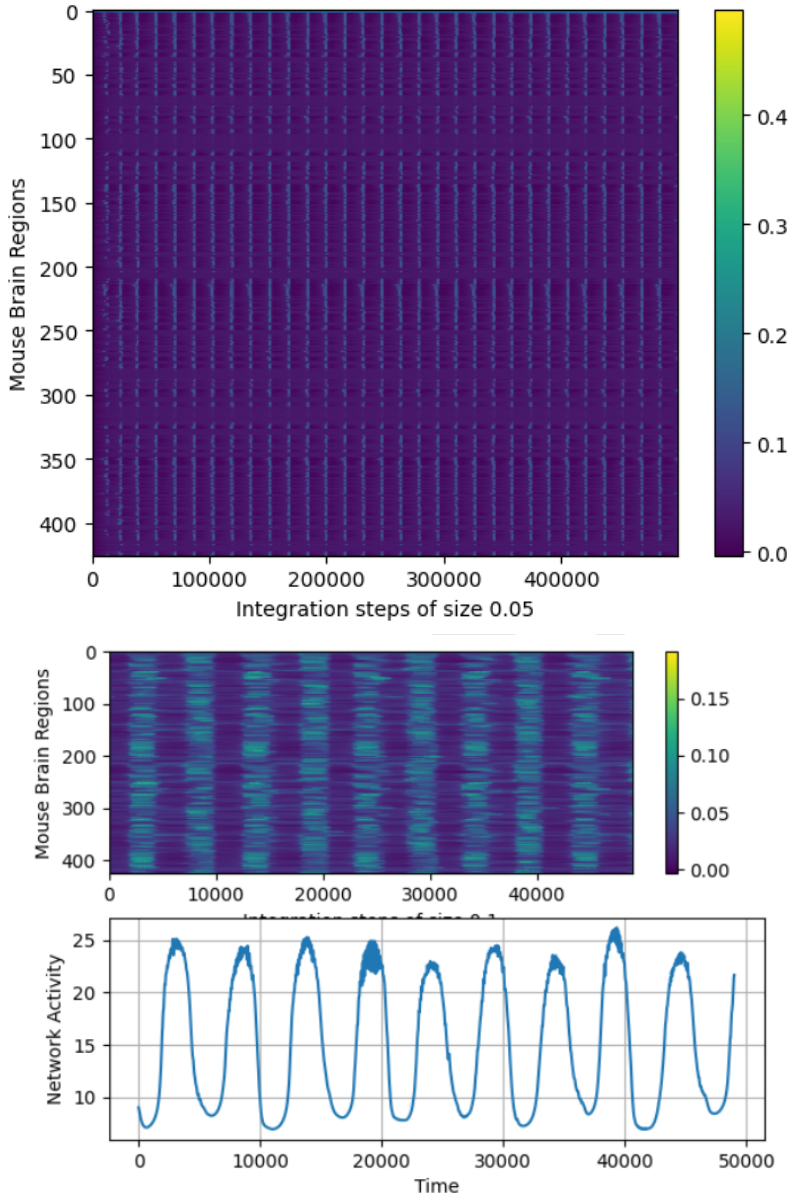

Fig. 5. The whole mouse brain seizure is shown. This activity is also reminiscent of the mouse brain under the effect of the anaesthesia due to, for example, barbiturates. Also, the state of unconsciousness is not only attributed to the coma or anaesthesia. The NME can also produce unconscious effects. This is what he model predicts. The EEG of the whole brain activity shall be a slow wave. The parameters used are the same as in (13). Global Coupling strength is 0.15.

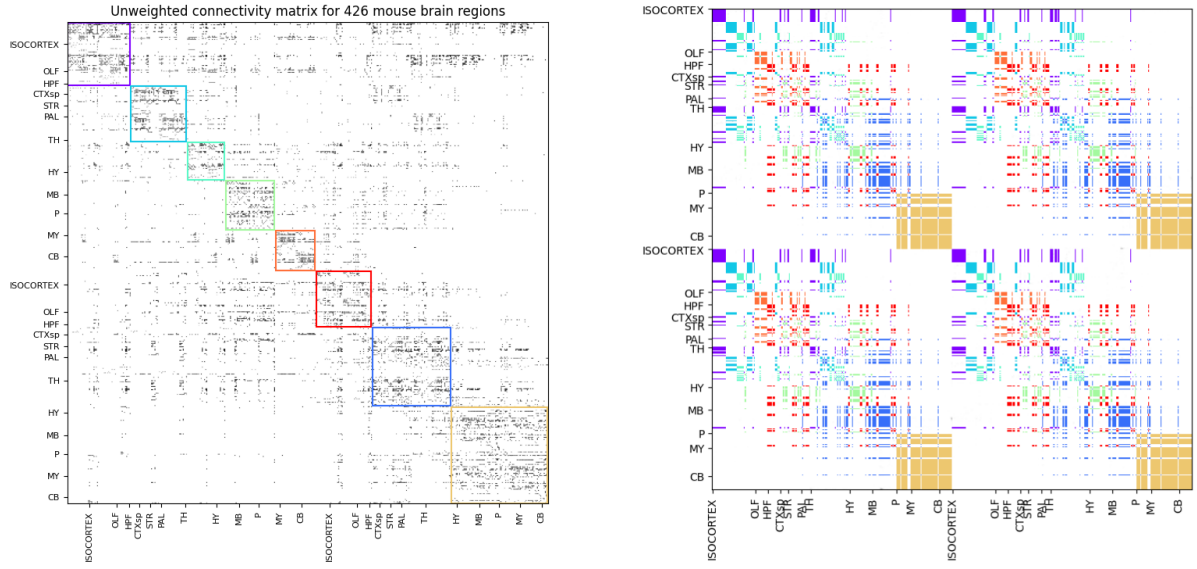

Fig. 6. Mouse brain Connectivity matrix. Each marker indicates a mouse brain region. Each dot is a link/connection. Ipsilateral connections are more in number than the contralateral connections. Global strength in calculations is between 0 and 1 (mostly 0.15)